12-20-2002

On the effect of random errors in gridded bathymetric compilations

Martin Jakobsson
Stockholm University

Brian R. Calder
University of New Hampshire, Durham, brian.calder@unh.edu

Larry A. Mayer
University of New Hampshire, larry.mayer@unh.edu

Recommended Citation
Jakobsson, M., B. Calder, and L. Mayer, On the effect of random errors in gridded bathymetric compilations, J. Geophys. Res., 107(B12), 2358, doi:10.1029/2001JB000616, 2002

On the effect of random errors in gridded bathymetric compilations

Martin Jakobsson, Brian Calder, and Larry Mayer

Center for Coastal and Ocean Mapping and Joint Hydrographic Center, University of New Hampshire, Durham, New Hampshire, USA

Received 18 October 2001; revised 8 January 2002; accepted 13 January 2002; published 20 December 2002.

[1] We address the problem of compiling bathymetric data sets with heterogeneous coverage and a range of data measurement accuracies. To generate a regularly spaced grid, we are obliged to interpolate sparse data; our objective here is to augment this product with an estimate of confidence in the interpolated bathymetry based on our knowledge of the component of random error in the bathymetric source data. Using a direct simulation Monte Carlo method, we utilize data from the International Bathymetric Chart of the Arctic Ocean database to develop a suitable methodology for assessment of the standard deviations of depths in the interpolated grid. Our assessment of random errors in each data set are heuristic but realistic and are based on available metadata from the data providers. We show that a confidence grid can be built using this method and that this product can be used to assess reliability of the final compilation. The methodology as developed here is applied to bathymetric data but is equally applicable to other interpolated data sets, such as gravity and magnetic data. *INDEX TERMS:* 0910 Exploration Geophysics: Data processing; 3045 Marine Geology and Geophysics: Seafloor morphology and bottom photography; 4536 Oceanography: Physical: Hydrography; 9315 Information Related to Geographic Region: Arctic region; *KEYWORDS:* bathymetry, Arctic Ocean, IBCAO, errors, Monte Carlo, grid

Citation: Jakobsson, M., B. Calder, and L. Mayer, On the effect of random errors in gridded bathymetric compilations, *J. Geophys. Res.*, *107*(B12), 2358, doi:10.1029/2001JB000616, 2002.

1. Introduction

[2] There is a growing demand in the geophysical community for better regional representations of the world's bathymetry. Researchers dealing with sea level change, ocean circulation, sediment transport, seafloor spreading, and modeling of ice sheets all require information on the shape of the seafloor. While multibeam sonar systems are filling hydrographic databases with relatively accurate bathymetric data sets from specific target areas, the quantity of observations being collected in most of the deep oceans (particularly remote areas) remains relatively small. The accuracy and resolution achievable with modern sonars are far better than that obtained with older single beam systems particularly considering the recent improvements in ship positioning. However, given the vastness of the oceans and the relatively limited coverage of even the most modern mapping systems, it is likely that many of the older data sets will remain part of our cumulative database for several more decades. Given this reality, regional bathymetric compilations that are based on a mixture of historic and contemporary data sets will remain the standard for the production of bathymetric charts. This raises the problem of assembling such bathymetric compilations and utilizing data sets with both a heterogeneous cover and a wide range of accuracies [*Bernardel*, 1997; *Macnab and Jakobsson*, 2000].

0148-0227/02/2001JB000616$09.00

[3] We address the issue of compiling bathymetric data sets with heterogeneous cover and a range of accuracies in the context of generating regularly spaced grids. For generating the grid we are often forced to use a complex interpolation scheme due to the sparseness and irregularity of the input data points. Consequently, we are faced with the difficult task of assessing the confidence that we can assign to the final grid product, a task that is not usually addressed in most bathymetric compilations.

[4] Traditionally, the hydrographic community has, after processing for outliers, cross-track analysis, etc., considered each sounding put on a chart as equally accurate and there has been no error evaluation accompanying the bathymetric end product. This has important implications for use of the gridded bathymetry, especially when it is used for generating further scientific interpretations. The method we describe is equally valid for the compilations of any other gridded data that are based on multiple sources with varying densities and accuracies (e.g., magnetic data, gravity data, etc.) where a random error component will remain in the source data after preprocessing.

[5] We approach the problem of assessing the confidence of the final bathymetry gridded product via a direct simulation Monte Carlo method. We start with a small subset of data from the International Bathymetric Chart of the Arctic Ocean (IBCAO) grid model [*Jakobsson et al.*, 2000] (Figure 1). This grid is compiled from a mixture of data sources ranging from single beam soundings with available

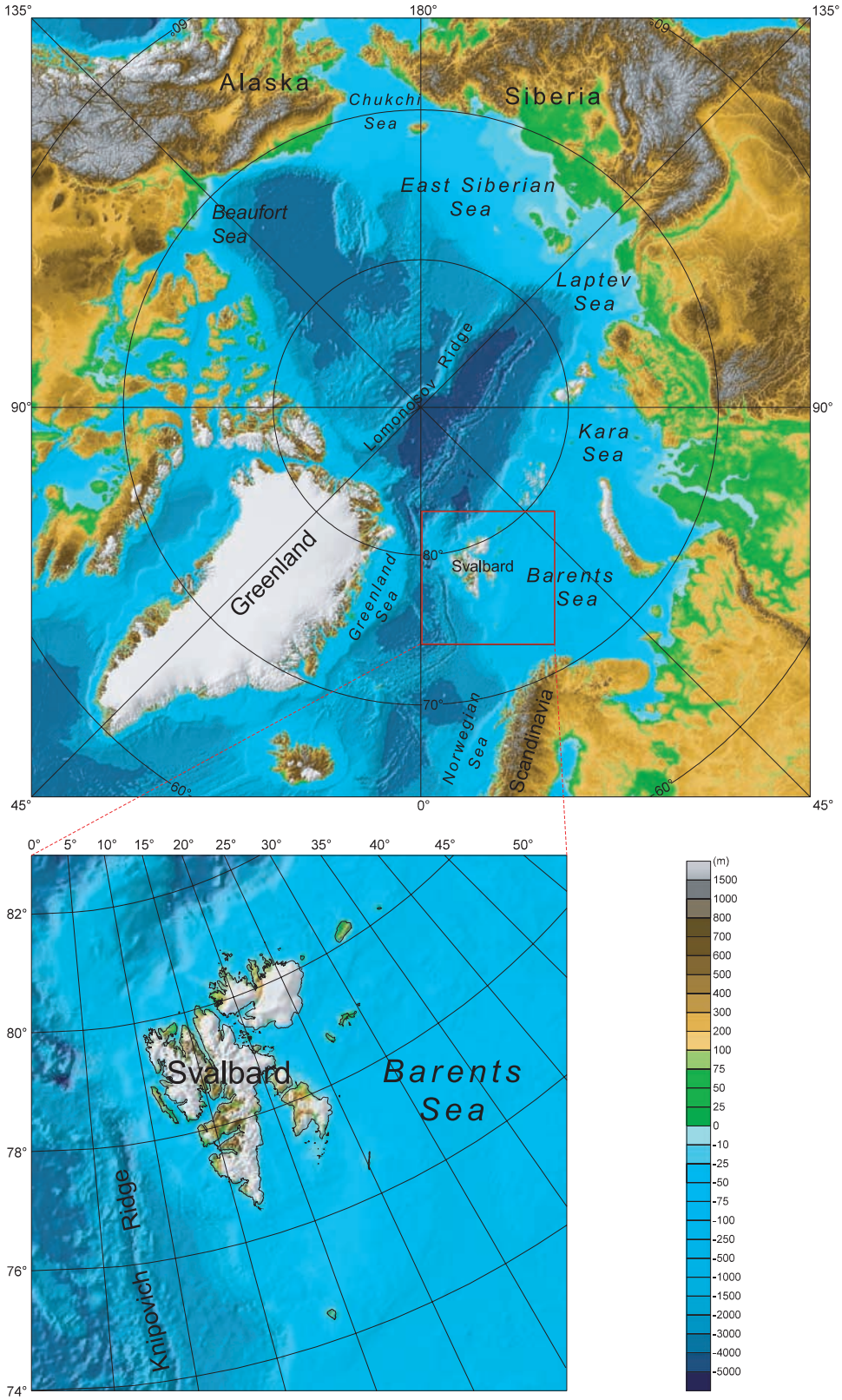

Figure 1. A color-coded shaded relief portraying bathymetry and topography of the Arctic region created from the IBCAO 2.5 km grid model. The area subjected to our error modeling experiment is indicated by a bold rectangle. Projection: Polar Stereographic with true scale at 75°N. Datum: WGS-84.

metadata, to spot soundings with no available metadata, to digitized contours; the test data set shows examples of all of these types.

[6] The IBCAO grid model source data has (like most hydrographic data) been preprocessed (section 2.1) to remove identifiable systematic errors, so that we believe that the only remaining error sources are random errors intrinsic in the measurements themselves. To this source database, we assign a priori error variances based on available metadata (i.e., data describing the source data, such as navigation and depth measurement system types), and when this is not available, based on a worst-case scenario in an essentially heuristic manner. We then generate a number of synthetic data sets by randomly perturbing the source data using normally distributed random variates, scaled according to the predicted error model. These data sets are next regridded using the same methodology as the original product, generating a set of plausible grid models of the regional bathymetry that we can use for standard deviation estimates. Finally, we repeat the entire random estimation process and analyze each run's standard deviation grids in order to examine sampling bias and standard error in the predictions. The final products of the estimation are a collection of standard deviation grids, which we combine with the source data density in order to create a grid that contains information about the bathymetric model's reliability.

2. Data Description

2.1. Implementation of the IBCAO Grid Model

[7] The International Bathymetric Chart of the Arctic Ocean (IBCAO) was initiated during 1997 in St. Petersburg, with the goal of collecting all available data north of 64°N [*Macnab and Nielsen*, 1999]. One of the major goals was to compile a regular grid model from the data collected within IBCAO. The IBCAO data consists of digital information that was obtained during recent icebreaker and Science Ice Expeditions (SCICEX) submarine cruises [*Rothrock et al.*, 1999] and older digital information that consists of recently declassified soundings collected between 1957 and 1988 by submarines of the U.S. and U.K. navies, and of observations obtained from the public domain archives of world and national data centers. In addition, hydrographic charts and compilation maps (portraying depth in the form of point soundings and hand-drawn contours) published by the Russian Federation Navy [*Department of Navigation and Oceanography*, 1999], by the U.S. Naval Research Laboratory [*Perry et al.*, 1986; *Cherkis et al.*, 1991; *Matishov et al.*, 1995], and by other agencies, were digitized using "heads up" digitizing techniques (a semi-automatic process of digitizing a scanned bathymetric chart) to supplement the original bathymetric measurements in the IBCAO data base.

[8] The IBCAO grid model also contains topography that was derived mainly from the USGS GTOPO30 topographic model [*U.S. Geological Survey*, 1997], with the exception of Greenland where the topographic model developed by KMS, the Danish National Survey and Cadastre, was used [*Ekholm*, 1996]. In order to constrain the coastline the World Vector Shoreline (WVS) [*Soluri and Woodson*, 1990] was used in all areas except Greenland and northern Ellesmere Island, where an updated coastline was made available by KMS.

[9] Initially, the original bathymetric soundings were corrected for sound speed in water using Carter's tables, or CTD profiles where available. After sound speed corrections, a suite of tools and statistical routines based upon the Helical-Hyperspatial (HH) scheme for data encoding [*Varma et al.*, 1990] was used to flag data as unusable if they were found to not statistically conform to nearby data. After this initial statistical cleaning all data (digitized bathymetric contours, land and marine relief grids, point, profile and swath observations, and vector shorelines) were imported into Intergraph's GIS Software, MGE (Modular GIS Environment). Polar stereographic projection on the WGS 1984 ellipsoid was used, with true scale at 75°N. For data sets derived from icebreaker data, it is often the case that there are large clusters of observations gathered during active ice breaking when headway is limited, and thus very dense soundings are collected in a very small area. To avoid these being overemphasized in the compilation, the observations along icebreaker ship tracks were sub-sampled to maintain a minimum of 500–1000 m between every point in each track. Soundings were color coded according to depth to facilitate a visual inspection of the statistical cleaning results. Outliers, cross-track errors, and the fit between isobaths and original observations were checked during this process. Further suspicious soundings were flagged, and where contours showed major discrepancies with soundings, the contours were adjusted manually to fit the new bathymetric track line data.

[10] After editing the entire Arctic Ocean bathymetry data set, the mixture of track and digitized contour values were used to construct a grid with a cell size of 2.5 × 2.5 km. The variable sampling density of the different data in the compilation led the IBCAO compilers to use an interpolated gridding algorithm, namely the continuous curvature spline-in-tension algorithm of *Smith and Wessel* [1990], as implemented in the GMT package [*Wessel and Smith*, 1991]. Prior to gridding the data was preprocessed by applying a block median filter with a block size equal to the final grid cell spacing of 2.5 × 2.5 km. This filtering serves the main purpose of preventing spatial aliasing. Finally, the GMT continuous spline-in-tension algorithm was used with the tension (T) parameter set to 0.35 in order to avoid overshooting in the interpolated regularly sampled surface. The resulting grid was inspected visually and problems identified. For example, a common problem was in narrow fjords without bathymetric data points where the gridding algorithm assigned 0 m values, the same value as the coastline. This was controlled by manually inserting control contours typically representing a depth of a few meters near the coastline, which conditioned the interpolation. A shaded relief of the entire IBCAO grid is shown in Figure 1. Further description about the IBCAO grid model is given by *Jakobsson et al.* [2000] and *Macnab and Jakobsson* [2000].

[11] We emphasize the preprocessing involved in the IBCAO compilation, a process which we include in our experiments here. As with all hydrographic data, preprocessing is implemented to remove the systematic errors and data outliers as well as they can be resolved (since such errors can be very significant [*Smith*, 1993]). Our

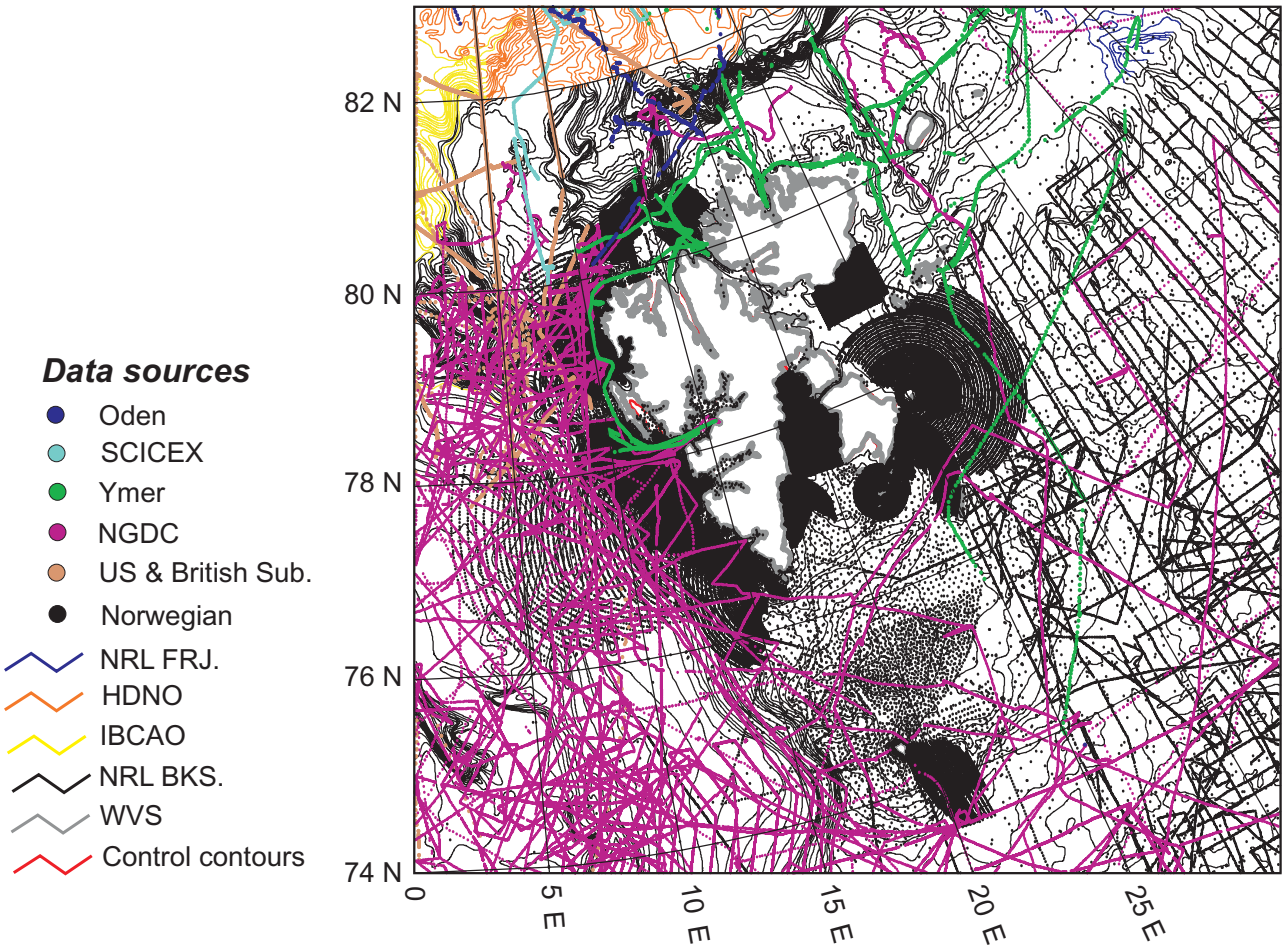

Figure 2. Data from the IBCAO construction database used for the error modeling. This includes all data that fall within the bounds indicated in Figure 1 and covers almost all of the component data sets used in the entire IBCAO grid compilation. Projection parameters are as in Figure 1. The key to the color coding of the source data is found in Table 1.

aim here is to show that irrespective of how well this preprocessing is done, there are still random errors inherent in the data. These errors will always affect the end product, but their effect has not been addressed previously.

2.2. Experimental Subset of IBCAO

[12] Our experiment is based on a subsection of the data used to construct the IBCAO grid, as shown in Figure 1. We have chosen the area around Svalbard since it contains a cross-section of the various régimes within the IBCAO source data, including nearshore regions, dense single-beam data, transect lines, bathymetric contours and control contours. There is also a significant depth range due to the relatively shallow areas of the Barents Sea around Svalbard and the contrasting deep of the Greenland Sea in the western part of the area where the Knipovich Ridge, the northernmost part of the North Atlantic Spreading Ridge, comes through. We have followed the exact same methodology as used for the construction of the IBCAO grid model. The data stored in the compilation database have been inspected and cleaned relative to the original data, and if not previously adjusted, the depths have been corrected for sound speed using Carter's tables. The resulting data set shows a distinct data density gradient from very dense survey data near Svalbard and in the southeast of the region to poorly constrained redigitized contours in the north and northeast (Figure 2).

3. Error Model

3.1. Methodology of Monte Carlo Simulation

[13] In principle, estimation of errors associated with the grid is a relatively simple matter. We need to gather a number of data sets for the same area (keeping track of the error sources in each), estimate depths in the area concerned, and then look at the variability in the depth estimates. However, in the regional case the vastness of the area and the difficulty and expense of collecting the data precludes repeated surveys. As an alternative, we consider an approximation of the error estimates required based on the best available data, our knowledge of the likely errors involved, and a simulation method.

[14] The Monte Carlo method [*Hammersley and Handscomb*, 1964; *Gentle*, 1998] is a numerical technique for

evaluation of difficult integrals, particularly where the integral is over multiple dimensions, or is otherwise complex to compute [*Brooks*, 1998; *Binder and Heerman*, 1988]. In the current context, the integrals of interest are the moments of random variables (i.e., depth at each grid node), which are constructed from a large number of data points using a complex iterative algorithm (as described above). The Monte Carlo method utilizes pseudo-random numbers to generate a set of simulations of a variable of interest (in this case the bathymetric grid surface) for which the statistical expectation is an estimate of the integral of interest (in this case the second central moment, or variance, of depth at a grid node) to within some numerical error. The flow-graph of our experiment is illustrated in Figure 3.

[15] Our computed value of standard deviation at any grid node is only an estimate of the true value due to our numerical approximation to the integral, and the magnitude of the error is a function of the number of random samples that we use in the approximation. We estimate the magnitude of this sampling error through multiple runs of the simulation. It is important to distinguish carefully between estimated standard deviation of the computed bathymetry (the target of the simulation) and the summary of the sampling distribution of the standard deviation grids (i.e., the standard error of the standard deviation estimate), computed between different simulation runs. Although computed in a very similar fashion, the former exhibit true variation corresponding to the problem under investigation, while the latter is an artifact of the sampling approach to estimation.

[16] The first assumption made here is that the data sets and the measurements within them are independent of each other and that they are free of any systematic bias. In this case, we can use the data points given as a basis for all of the pseudo-data sets, perturbing about the values supplied. In effect, we assume that the points recorded are unbiased estimates of the mean bathymetry and position. The only location where this might not be justified is in the region of the Barents and Kara seas, where some track lines present in the database might have been used to form the contours that were subsequently redigitized for IBCAO. There is currently no way to verify this due to limitations in the amalgamated source databases. This is, however, only a very small part of the compilation, and we do not believe the effect to be significant.

[17] Our other principal assumption is that the random errors in location and depth are normally distributed, independent of each other and of each data point. This assumption is more weakly justifiable, since we may have some systematic bias in navigation (e.g., a poorly navigated submarine track 10 km from the true location). In all detectable cases, however, these have been resolved in the preprocessing stage and should not concern us here. We may also have some correlation between the two horizontal offsets. However, such fine detail is essentially unknown and unknowable in the data sets we are considering, and we are forced, reluctantly, to accept this assumption in order to carry out the analysis.

[18] In a similar vein, we note that this analysis does not give us any more insight into the error budget for the grid than a full formal error analysis would. However, it does provide a very simple way to carry out what would otherwise be a very complex computation. Pragmatically, we trade off accuracy for tractability.

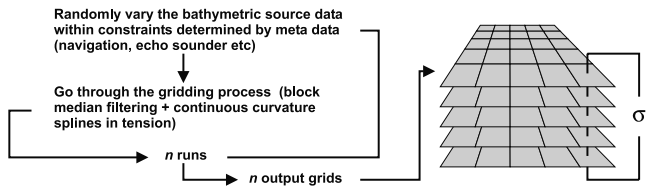

Figure 3. Conceptual organization of the Monte Carlo method applied to error estimation. Errors are estimated via sample statistics computed pointwise over pseudo-randomly generated grids.

3.2. Estimation of Errors in the IBCAO Source Data

3.2.1. Track Lines

[19] Our error modeling approach is based on an assumption of normally distributed random errors in the source data. In the case of bathymetric data this may be subdivided into errors in determining position (x, y) and errors in measuring depths (z). We model (x, y) errors in terms of meters, but model z error as a percentage of measured depth [*IHO Committee*, 1996]. A more detailed model of errors (e.g., [*Hare et al.*, 1995]) would be preferable, but essentially impossible to configure given the lack of metadata for these data sets. For recently collected survey data an estimate of the random errors and possible constant errors (which then can be corrected) may be available from those who collected the data. However, in the case of the IBCAO source data, the majority of the data sets are historic. Thus, only the metadata is available to make a realistic initial random error assumption, although recent studies have attempted to address the random error in position for radio positioning error [*Calderbank*, 2001]. If there is no metadata available the assigned errors must be based on a worst-case scenario in order to highlight this uncertainty. The most critical information in the metadata is type of positioning/navigational instrumentation, bathymetric instrumentation and year. Other information like geodetic datum and sound speed correction would also contribute to the initial error assignment if available. From the metadata the random error is estimated at a selected confidence interval, in this case 95%. This means that 95% of the normally distributed positions should fall within a circle with a radius of the assigned error.

[20] It is not a straightforward task to assign an error simply based on the metadata, but it is the only approach possible for historic data sets. For example, if it is found that the positions were acquired using a GPS system during 1990, the random error may be on the order of ±80 m [*Wells et al.*, 1986]. However, if positions were acquired using Loran C, error characterization is more complicated because its accuracy varies more widely with time and location [*Maloney*, 1985]. Again, the worst-case scenario is the easiest and safest approach. Constant errors are more problematic to account for in historic data sets, although they may possibly be distinguished through crossing track lines.

3.2.2. Contours and Associated Problems

[21] The contour is still the traditional means of displaying bathymetry. In theory, a contour represents exactly one value along its entire extension. However, in reality, con-

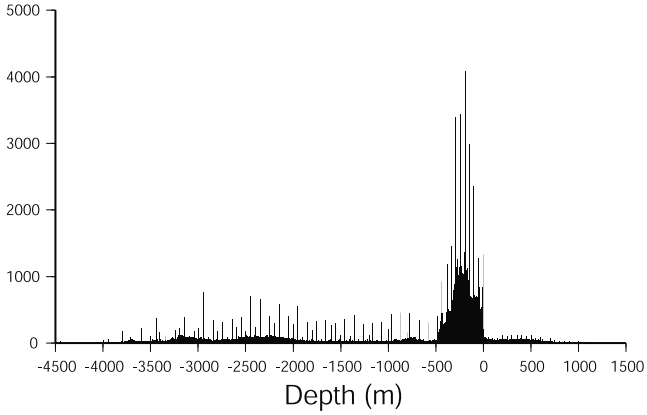

Figure 4. Histogram of the grid node depths in the subsection of the IBCAO model shown in Figure 1. The spikes are caused by a bias toward the depths as represented by contours in the source data.

tours are typically interpolations based on underlying sparse ship track data. Therefore, the depth is only true where the contour crosses a track line. Without the source data and its associated metadata being available, it is not possible to judge the accuracy of the bathymetric contours. In addition, a manually derived contour map will inherit a style from the cartographer/geophysicist who drew it. All this makes it difficult to produce an error estimation of a bathymetric contour map. When contours are used as source data for creating a gridded surface these problems go along with it. In addition, a gridding algorithm suitable for interpolating a regular grid from the contours is required [*Smith and Wessel*, 1990]. For example, terracing is an artifact in grid models that arises from gridding source data that consists primarily, or in parts, of digitized contours. The terracing is due to a bias toward the contour values. If artificial illumination is applied to a gridded surface suffering from terracing the surface shows steps between terraces at the contour values. The IBCAO grid shows some terracing along the central Arctic Ocean continental slopes where digitized contours dominate. A histogram of depths of the gridded surface's nodes clearly reveals a bias toward the digitized contours (Figure 4).

3.2.3. Error Assignment

[22] Some of the data sets within the IBCAO source data have no metadata associated with them. However, in our error modeling experiment, which is focused on developing the modeling approach rather than producing the best possible estimate of the errors in the subset of the IBCAO grid around Svalbard, we have assigned generalized errors to all data sets based on the classification described in Table 1. Contours are assumed to have the largest errors whereas the data from the Norwegian sources, which mainly consists of hydrographic survey data is the lowest. Data from the R/V *Oden* collected using GPS positioning is considered to have the highest horizontal accuracies. The data collected from submarines are considered to be inaccurately positioned (±5000–10000 m) due to the use of inertial navigation for long periods between surface fixes. The data collected from the R/V *Ymer* was positioned using a Magnavox one-channel satellite system [*Eldholm et al.*, 1982], which we have assigned an accuracy on the order of ±1 nm. The data retrieved from the NGDC data center is assigned common positional and depth errors. A full error estimation of the entire IBCAO grid is one of our future goals. This will require a large amount of time-consuming "data detective" work in order to find metadata (i.e., descriptions of the data sets, for example the type of positioning system) for many of the

Table 1. Classification of the Source Data Shown in Figure 2 and Initial Assignment of Standard Deviation of Errors at 95% Confidence Interval

Source data	Horizontal Error, m	Vertical Error, % Depth
Digitized Contours		
Contours drawn during the IBCAO project (yellow)	12,000	5
Bathymetry of the Franz Josef land area [*Matishov et al.*, 1995] (blue)	12,000	5
Bathymetry of the Barents and Kara Seas [*Cherkis et al.*, 1991] (black)	12,000	5
Bottom relief of the Arctic Ocean [*Department of Navigation and Oceanography*, 1999] (orange)	12,000	5
Soundings		
Swedish icebreaker *Oden*, 1991 and 1996 (blue)	100	5
Swedish icebreaker *Ymer*, 1980 (green)	1,852	5
U.S. and British Royal Navies submarines, 1958–1988 (brown)	10,000	5
Data collected during SCICEX by USS *Hawkbill*, 1999 (cyan)	5,000	5
Data from Norwegian sources (black)	200	2
Soundings obtained from the U.S. National Geophysical Data Center (NGDC) (magenta)	1,000	5
Land and Support Data		
World Vector Shoreline (gray)	0	0
Control contours (red)	0	0
GTOPO30 (blank)	0	0

older data sets. Only then will it be possible to assign errors that are more closely related to the ''true'' errors.

4. Data Preprocessing and Simulation

4.1. Preprocessing

[23] We used the bounds indicated in Figure 1 to extract the relevant data from the IBCAO compilation. Data are represented as flat-file (x, y, z) triples using projected coordinates and corrected depths.

4.2. Data Set Simulation

[24] The experimental estimation of standard deviations on the grids consists of a number of repeated simulations. In particular, we have to consider M sets of N grids. We therefore subscript all variables $\mathbf{A}_{nm}$ or $\mathbf{A}_m$ as appropriate, where upper case bold letters indicate matrices (or grids) and lower case bold letters indicate (column) vectors. Operations on grids are always taken pointwise (so $\mathbf{A} = \mathcal{F}(\mathbf{B})$ for some operator $\mathcal{F}(\cdot)$ means $A_{ij} = \mathcal{F}(B_{ij})\ \forall i,j$ on the domain). Sets of variables are indicated by sans serif letters, e.g., $\mathsf{Y} = \{\mathbf{Y}(1),\ldots, \mathbf{Y}(k)\}$; when appropriate, we refer to components of a set indexed over $\mathbb{N}$ (the set of natural numbers) with an essentially arbitrary, but fixed, indexing scheme.

[25] Given the collection of cleaned data sets $\mathsf{X} = \{\mathbf{X}(1),\ldots, \mathbf{X}(s)\}$ and a corresponding error model, $\mathsf{E} = \{\mathbf{e}(1),\ldots, \mathbf{e}(s)\}$, $\mathbf{e}(i) = [\sigma_x^2(i), \sigma_y^2(i), \alpha_0^2(i)]^T$, we generate a pseudo-data set X_{nm} by perturbing each sounding with a random vector as follows:

$$\mathsf{X}_{nm} = \{\mathbf{X}_{nm}(1), \ldots, \mathbf{X}_{nm}(s)\} \tag{1}$$

$$\mathbf{X}_{nm}(i) = \mathbf{X}(i) + \boldsymbol{\mathcal{E}}_{nm}(i) \qquad 1 \le i \le s \tag{2}$$

$$\boldsymbol{\mathcal{E}}_{nm}(i) = \left[\boldsymbol{\eta}_1(i), \ldots, \boldsymbol{\eta}_{J(i)}(i)\right]_{nm} \qquad J(i) = |\mathbf{X}(i)|,\ 1 \le i \le s \tag{3}$$

$$\boldsymbol{\eta}_j(i) \sim \mathcal{M}\left(\mathbf{0}, \mathrm{diag}\left(\sigma_x^2(i), \sigma_y^2(i), \alpha_0^2(i) z_j^2(i)\right)\right) \tag{4}$$

$$1 \le j \le J(i),\ 1 \le i \le s$$

where $\mathcal{M}(\boldsymbol{\mu}, \boldsymbol{\Sigma})$ is the multivariate normal distribution with mean $\boldsymbol{\mu}$ and covariance matrix $\boldsymbol{\Sigma}$.

[26] Gaussian variates are generated using the Box-Muller equations driven by a nonlinear congruential generator that is known to have sequence length of at least 2^{35} and produces equally random bits in all sections of the output word. The uniform variates are scaled to [0, 1) before conversion to Gaussian distributions.

[27] The basic component of the simulation is a block of $N = 100$ pseudo-data sets, from which we construct a set of N grids using the same algorithm as the IBCAO compilation, with a mask prepared from GTOPO30 topography to constrain the standard deviation estimate to be zero on land. We then compute the expectation $\mathbf{B}_m = \mathbb{E}[\mathbf{B}_{nm}]$ and the standard deviation $\boldsymbol{\epsilon}_m = \mathbb{E}[(\mathbf{B}_{nm} - \mathbf{B}_m)^2]$ of this set, the latter estimating our confidence in the former's depth prediction. Computations are done directly on the grids using the GMT grid calculator; this avoids any conversion errors or approximations. The standard deviation estimate $\boldsymbol{\epsilon}_m$ is the primary outcome of the simulation.

[28] To estimate the Monte Carlo error, we repeat the above basic simulation $M = 20$ times. We then compute the expectation $\bar{\boldsymbol{\epsilon}} = \mathbb{E}[\boldsymbol{\epsilon}_m]$ and standard error estimate $\boldsymbol{\epsilon} = \mathbb{E}[(\boldsymbol{\epsilon}_m - \bar{\boldsymbol{\epsilon}})^2]$ of the individual standard deviation grids, providing us with a spatially localized estimate of the variability of standard deviation at each estimation grid point.

5. Results

5.1. Standard Deviations in Gridding and Gridding Stability

[29] Standard deviation grids for a single run of the algorithm (i.e., $\boldsymbol{\epsilon}_m$) are shown in Figures 5a and 5b. We can visualize the error in two ways: either as true meters, or as a percentage of the depth estimated from the unperturbed data, X. Based on the assumption that we are more interested in relative errors, especially in the nearshore region, we will concentrate mainly on the percentage error grid (Figure 5b).

[30] On first examination, the results appear to agree with intuition. In regions where there have been rigorous hydrographic surveys (e.g., 77°N, 22°30′E), the estimated error is significantly lower than regions where only a single track line is used to constrain the grid (e.g., at 82°N, 5°E). We also clearly see that where there are track lines, the error is lower, and that inshore the error is proportionately higher.

[31] However, comparing the grids to the source data grid (Figure 2), we see some anomalies. For example, the region near 79°30′N 37°E has suspiciously low error given the scarcity of data in the area. We attribute this to the smoothing interpolative nature of the gridding algorithm and the fact that the source data in this region predominantly derives from contours. That is, in flat regions with little data enclosed by contours, what we see is a smooth approximation between the contour limits, rather than a realistic error estimate.

[32] Consequently, we chose to remove from consideration areas that are equal to or larger than 7500 × 7500 m that contain no soundings. The resulting reduced grid, with these areas shaded in gray, is shown in Figure 6, and by comparison with Figure 5b, we can see that the anomalous area described above is completely removed. We note that some variant of a combination of sounding density and different resolution grids may be a way to approach a prediction of the required gridding density for any particular data set, a topic we are currently investigating further.

[33] With the empty grid cells removed, we can interpret the results with more confidence. The major feature of the grid is the significantly increased error in regions of higher slope (Figures 6 and 7). This is principally due to problems of excessive horizontal error, which cause a significantly increased depth error as they shift slopes from place to place. This is also the case for the ridge of high error running from Bjørnøya (74°30′N, 19°E) to Svalbard, although the ridge is not as obvious in the bathymetry.

[34] Perhaps more surprising than the regions with significant errors is the remarkable uniformity of error over much of the shelf area to the southeast of Svalbard. This is due principally to the relatively even distribution of soundings over the entire area (which are mainly derived from Norwegian hydrographic survey data), in combination with the general lack of large relief in the area. If the region being studied were essentially flat on a suitably large horizontal scale, then it is immaterial how much horizontal error is

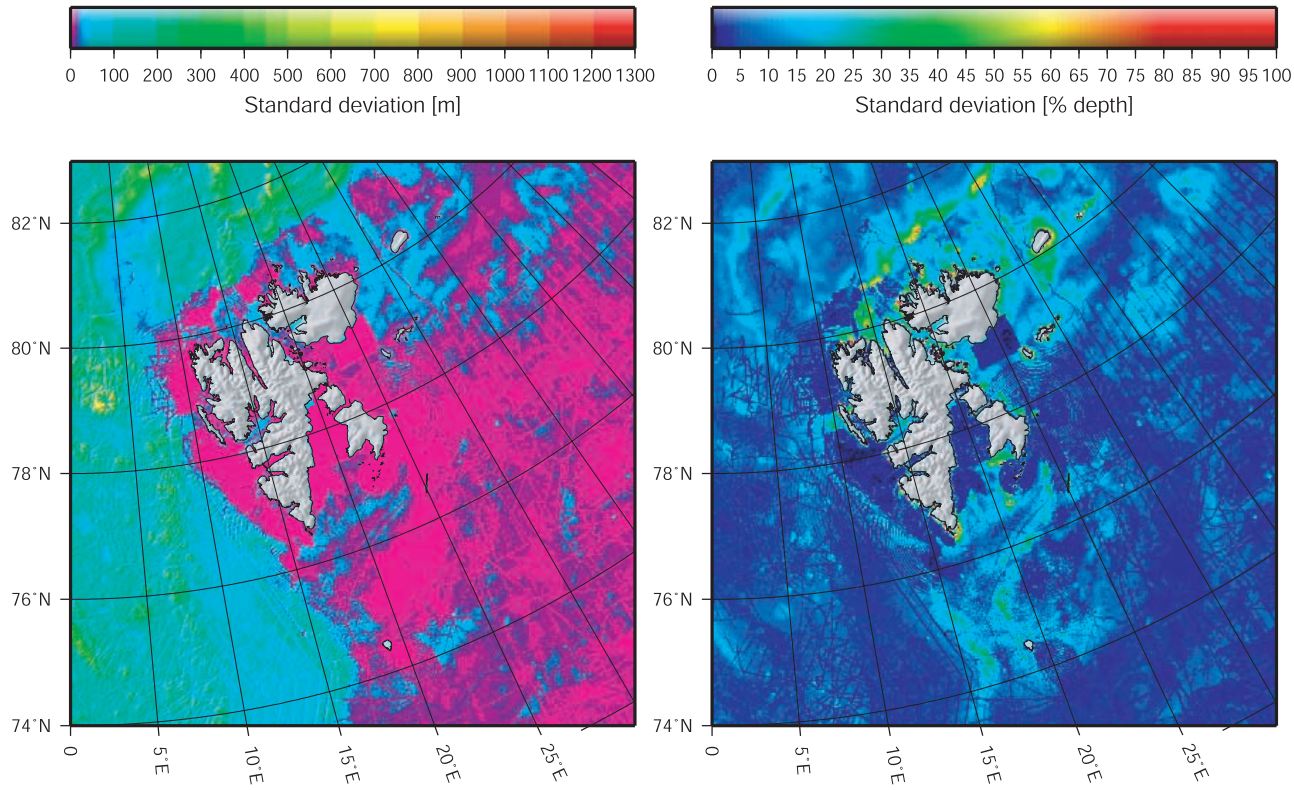

Figure 5. (a) Estimated standard deviation of gridded depth based on $N = 100$ Monte Carlo simulation runs. Standard deviation is depth in meters. (b) Estimated standard deviation of gridded depth based on $N = 100$ Monte Carlo simulation runs. Standard deviation is shown as a percentage of the depth estimated on the unperturbed grid. The percentage grid gives a better feel for the errors involved and is the preferred grid for interpretation.

found in the data; all soundings should indicate the same true depth, and hence the principal error source observed will come from vertical error in the sounding system, rather than from geographical variability coupled into the soundings through mislocation.

[35] The potential of this approach is demonstrated by the identification of the error associated with the seamounts at 82°N, 24°E (Figures 5a, 5b, and 7). The error estimate shows clearly that significant error is associated with the whole seamount, rather than just the slopes. Indeed, a profile of the gridded bathymetry across the feature shows a relief of approximately 1500–1700 m from the surrounding seafloor, and the estimated standard deviation is over 1000 m on the tops of the seamounts, suggesting that we would not be able to tell the seamounts from the background with any significant confidence (in the sense of a statistical test of the null hypothesis that there is no difference in depth between the background and the tops of the seamounts). This would be the case for any high relief feature defined by a single track line with poorly constrained navigation. A subsequent survey of the area by the R/V *Polarstern* [*Jokat*, 1999] showed that the feature did not really exist; further investigation of the original data (from the R/V *Oden*) found a malfunctioning echo sounder.

5.2. Monte Carlo Estimation Errors

[36] The estimate of Monte Carlo error, $\boldsymbol{\epsilon}$, is shown in Figure 8. Recalling that the purpose of this grid is to show regions of the target area where our prediction of standard deviation is more variable, we can see that most areas are estimated in a stable fashion, but that there is more variability in the deeper areas. We conjecture that this is simply due to the higher vertical error in deeper water, resulting in higher variability in the grids, and hence in both the standard deviation estimate and variability of that estimate.

[37] In practice (in this data set), the relative error in the estimation is slight. We could reduce the Monte Carlo error by generating more pseudo-random grids, or by agglomerating two or more of the independent runs. However, this only reduces the error slowly, and in this case is probably not warranted.

6. Discussion

6.1. Assessment of Methodology

[38] As described previously, our numerical approximation to error estimates does not give us any more information than a formal error propagation analysis of the gridding algorithm would provide. However, we also observe that such a formal analysis would be very difficult (or impossible) to carry out under the circumstances, and hence the approximation here is justified. Given the assumptions inherent in the method, our results show that the technique generates results in line with intuition and common sense. However, the assumptions that we have made do limit the applicability of the method as it stands.

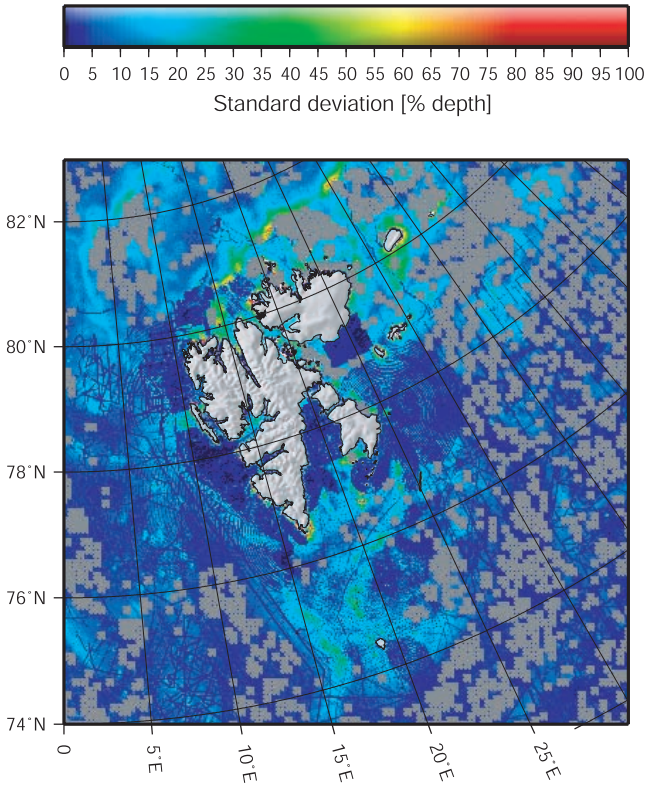

Figure 6. Standard deviation grid (percentage of estimated depth) with empty grid cells removed. Interpretation of standard deviation in the grid where there is no data is essentially a function of the interpolation surface used in gridding, rather than actual errors caused by variability of data. We remove empty cells to avoid overinterpretation in sparse data.

[39] We have assumed that our input data was preprocessed for systematic errors, and only random errors need to be modeled. This is implicit in the use of normally distributed random variates to generate the pseudo-independent data sets used in the Monte Carlo estimation. Although we believe that this is the most likely error mode for the data once it is cleaned and entered into the database, it is not the only error mode possible. In particular, we could encounter a survey line that is very badly navigated, for example due to long-term drift in inertial navigation systems. In this case, a systematic bias has been introduced into the data and our assumption that the recorded data is a valid estimate of the population mean is violated. However, it is impossible to identify these types of errors without further cross checks (such as the repeated observations which highlighted the problem with the pseudo-seamounts in this work), and we consider the identification of such errors beyond the scope of our statistical error assessment. A cross track analysis and correction of data sets that are offset due to poor navigation should be performed prior to the gridding; there are several possible approaches to this problem [e.g., *Caress and Chayes*, 2000; *Smith*, 1993].

[40] We have assumed that random errors in the source data are distributed as Gaussian random variates, and that the variance is the same for all points in each component data set. Lacking a more formal assessment of the errors associated with each data set, this is probably unavoidable. Indeed, with historical data sets, it may be difficult to determine reasonable errors with any certainty since the metadata describing the instrumentation package may not be adequate (or extant). As we have done here, future work will have to assign subjective (but informed) error bounds, making sure to err on the side of caution and assess slightly exaggerated errors. Studies of the accuracies of positioning systems [e.g., *Calderbank*, 2001] will be important in this endeavor. Since the principal goal of the research is to inform users as to the trust they can have in the generated grid data, too high an error assessment is preferable to an underestimate. The assignment of the initial errors bounds to the data sets, which is fundamental for our modeling approach, will be one subject of further research. During the past century, depth and positioning measurements have gone from lead lines to multibeam sonars and from sextants to differential GPS. Each advance in technology is associated with a tremendous improvement in the accuracy and resolution. Considering the technology used for bathymetric data collection, a thorough classification in terms of random errors may be done. However, there are also other factors, more difficult to discern, that may add to the random errors of the collected data, including weather conditions and human factors.

[41] Finally, we have assumed that the IBCAO gridding algorithm is the right way to compute the gridded product. In terms of comparing the error assessment with the original data this is unavoidable, but it is certainly a limiting factor to the application of the methodology to other data sets. However, nothing in the theoretical foundation of the technique we describe requires that the IBCAO gridding model is used, and substitutions may be made on a black-box basis. The principal shortcoming of the methodology outlined is that it is difficult to discriminate between low errors arising from accurate data, and low errors arising from gridding artifacts where there is low data density. This is typically associated with areas defined principally through contour data, which also causes significant terrac-

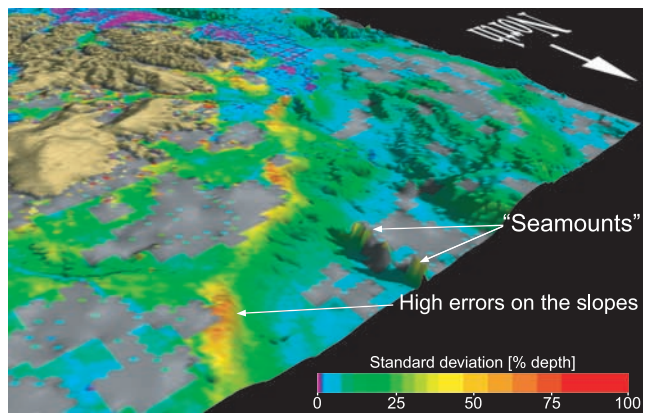

Figure 7. Three-dimensional image, created using the Fledermaus software, showing the standard deviation as a percentage of the depth estimated on the unperturbed grid and draped on the IBCAO bathymetry. The error estimate shows clearly that significant error is associated with the indicated seamounts later revealed not to exist by a survey with R/V *Polarstern*.

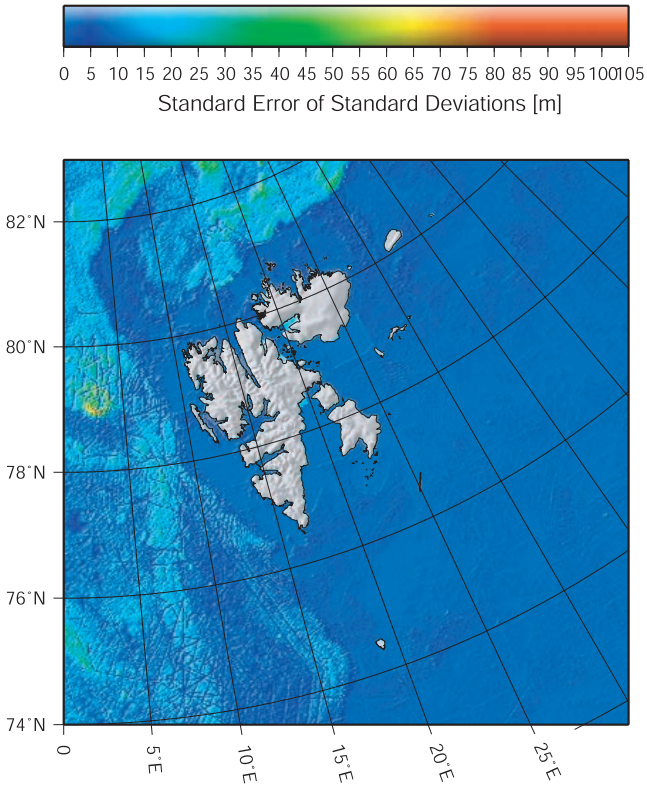

Figure 8. Estimate of Monte Carlo error associated with the standard deviation estimates. This grid is estimated as the sampler error associated with the standard deviation estimates, computed over $M = 20$ example standard deviation grids.

ing in the bathymetry. Although we can avoid this problem by removing from consideration areas with low data density, it would be better to avoid contours whenever possible and instead use the original source data. The need to rely on contour-only derived data is probably most acute in the Arctic where the strategic sensitivity of data sources has resulted in a general reluctance to distribute original sounding data.

[42] Related to the problem of density is one of resolution, which we have not really considered in the present work. That is, at what grid resolution should we work, and should this be the same across the entire grid? Determination of a reasonable resolution at which to work is essential, particularly to ensure that we are making interpretations correctly when we look at error estimates. Ideally, we should work at a resolution determined by the spatial frequencies associated with the bathymetry in question, and have data-driven grid cells. In practice, the spatial frequency spectrum of the bathymetry is not known a priori, and we have to resort to some approximation, such as reducing the resolution and repeating the error estimation until our standard errors stabilize. We would then be able to use the stabilization resolution as a local working resolution for further work. Assessment of stability of the estimation also informs us about the highest resolution that is reasonable for interpretation of the data in question; and this is not necessarily stable across the grid when we have many different vintages of data sets. We consider that the issue of gridding resolution is the most significant outstanding issue with the current methodology, and are actively pursuing improvements in this area.

[43] One of our initial goals was to create an error assessment in the same format as the bathymetry grid. The reason for this is to prevent overinterpretation of the bathymetry by facilitating the visualization of the errors associated with the gridded data set in modern GIS tools and other grid analysis software. The standard deviation error associated with each depth in a grid cell may be represented as an attribute to the bathymetric depth. In Figure 7 the form of the three-dimensional (3-D) surface visualizes the morphology of the sea bottom while the color coding represents the standard deviation error (as a percentage of depth) in each grid cell. In this way the relationship between the uncertainty of the bathymetry and the regional morphology can clearly be seen. Such an approach allows for the intuitive interpretation of potential sources of uncertainty. We have limited our error modeling to bathymetry. However, this approach may be applicable to other geophysical data sets such as gravity and magnetics that exist as gridded data compiled using similar approaches as we used for the IBCAO bathymetry grid [*Verhoef et al.*, 1996; *Laxon and McAdoo*, 1994].

[44] Finally, we note that our approach could also be used to address the uncertainty of a derivative product of a grid model, for example isobaths built from a bathymetric surface. An example is the isobath at 2500 m, which is used by nations in the process of making a claim under Article 76 of the United Nations Convention on the Law of the Sea (UNCLOS). Stacking isobaths generated from each of the Monte Carlo bathymetric grids could provide an estimate of the variability in positioning of the 2500 m isobath due to random errors in the source data, and hence in variability of the potential claim [*Jakobsson et al.*, 2001].

7. Conclusions

[45] We conclude that the prediction of accuracies in final gridded bathymetric products is possible using a Monte Carlo approach, with the added advantage that the output error assessment is in the same form as the original gridded product. Our predictions on a test data set agree with common sense, and provide important caveats on the use of gridded data products. Our experiments clearly show areas of high certainty associated with the more accurate data in the data set, and regions which are less reliable, typically associated with contour-based data. We also discovered areas of unexpectedly high uncertainty, which we subsequently found to be associated with erroneous data from a single track line.

[46] We have outlined a methodology for the assessment of errors in gridded bathymetric data sets. Although the method has been applied to the problem of sparse data sets requiring interpolation, we believe that it can also be applied to other types of data. However, there may be alternatives when data is denser, for example when dealing with multibeam echo sounder data. The methodology relies on essentially subjective assessments of the errors associated with the data sets used. It would be preferable to assign errors based on a more formal model of the data gathering equipment, but these are often not available. In many cases, the

subjective but conservative estimate of an experienced observer may be more useful than the alternatives.

[47] We have essentially neglected the issue of resolution in this analysis, although it is probably a significant constraint, especially in sparse data. The resolution at which data is analyzed should be data-driven, rather than specified *a priori*. However, implementation and theoretical difficulties involved in this are not trivial, and are currently the subject of further research.

[48] **Acknowledgments.** We thank Magnus Mörth for coming up with the idea that the Monte Carlo method might be useful for our error modeling of bathymetric data. We would also like to thank the Associate Editor and two anonymous reviewers for comments that significantly improved the manuscript. We gratefully acknowledge NOAA grant NA970G0241 for supporting this project.

References

Bernardel, G., Digital terrain model for the Tasmanian region: A pilot study into combining disparate datasets, *Tech. Rep. AGSO Rec. 1997/61*, Aust. Geol. Surv. Org., Canberra, 1997.

Binder, K., and D. W. Heerman, *Monte Carlo Simulation in Statistical Physics*, Springer-Verlag, New York, 1988.

Brooks, S. P., Monte Carlo Markov Chain method and its applications, *Statistician*, *47*(1), 69–100, 1998.

Calderbank, B., Radio positioning accuracies, *Lighthouse, Spring/Summer*, 12–15, 2001.

Caress, D., and D. Chayes, Optimal navigation adjustment for poorly navigated swath bathymetry surveys, *Eos Trans. AGU*, *81*(48), Fall Meet. Suppl., Abstract T52C-14, 2000.

Cherkis, N. Z., H. S. Fleming, M. D. Max, P. R. Vogt, M. F. Czarnecki, Y. Kristoffersen, A. Midthassel, and K. Rokoengen, Bathymetry of the Barents and Kara Seas, scale 1:2,313,000, *Geol. Soc. Am. Map Chart Ser.*, *MCH047*, 1991.

Department of Navigation and Oceanography, Bottom relief of the Arctic Ocean; map, scale 1:5,000,000., All Russ. Res. Inst. of Sci., St. Petersburg, Russia, 1999.

Ekholm, S., A full coverage, high-resolution, topographic model of Greenland computed from a variety of digital elevation data, *J. Geophys. Res.*, *101*, 961–972, 1996.

Eldholm, O., E. Sundvor, M. Sand, and K. Crane, *YMER-80: Navigation and Bathymetry*, Univ. i Oslo, Oslo, 1982.

Gentle, J. E., *Random Number Generation and Monte Carlo Methods*, Springer-Verlag, New York, 1998.

Hammersley, J. M., and D. C. Handscomb, *Monte Carlo Methods*, Methuen, New York, 1964.

Hare, R., A. Godin, and L. A. Mayer, Accuracy estimation of Canadian swath (Multibeam) and sweep (MultiTransducer) sounding systems, technical report, Can. Hydrogr. Serv., Ottawa, 1995.

IHO Committee, IHO standard for hydrographic surveys, *Spec. Publ. 44*, 4th ed., Int. Hydro. Org., Monaco, 1996.

Jakobsson, M., N. Z. Cherkis, J. Woodward, B. Coakley, and R. Macnab, A new grid of Arctic bathymetry: A significant resource for scientists and mapmakers, *Eos Trans. AGU*, 81(9), 89, 93, 96, 2000.

Jakobsson, M., B. Calder, L. Mayer, and A. Armstrong, The uncertainty of a bathymetric contour: Implications for the cut-off line, in *Acuracies and Uncertainties in Maritime Boundaries and Outer Limits*, *ABLOS Conference* [CD-ROM], Int. Hydrol. Bur., Monaco, 2001. (Available at http://www.gmat.unsw.edu.au/ablos/).

Jokat, W., The Expedition ARKTIS-XV/2 of Polarstern, *Tech. Rep. 368-2000*, Alfred-Wegener Inst., Bremerhaven, Germany, 1999.

Laxon, S., and D. McAdoo, Arctic ocean gravity field derived from ERS-1 satellite altimetry, *Science*, *265*(5172), 621–624, 1994.

Macnab, R., and M. Jakobsson, Something old, something new: Compiling historic and contemporary data to construct regional bathymetric maps, with the Arctic Ocean as a case study, *Int. Hydrol. Rev.*, *1*(1), 2–16, 2000.

Macnab, R., and A. Nielsen, IOC/IASC editorial board for the International Bathymetric Chart of the Arctic Ocean, *Open File Tech. Rep. 3713*, Geol. Surv. of Can., Ottawa, 1999.

Maloney, E. S., *Dutton's Navigation and Piloting*, 14 ed., Nav. Inst. Press, Annapolis, Md., 1985.

Matishov, G. G., N. Z. Cherkis, M. S. Vermillion, and S. L. Forman, Bathymetry of the Franz Josef land area, *Geol. Soc. Am. Map Chart Ser., MC-56*, 1995.

Perry, R. K., H. S. Fleming, J. R. Weber, Y. Krisoffersen, J. K. Hall, A. Grantz, G. L. Johnson, N. Z. Cherkis, and B. Larsen, Bathymetry of the Arctic Ocean, map, scale 1:4,704,075, *Geol. Soc. Am. Map Chart Ser., MC-56*, Boulder, Colo., 1986.

Rothrock, D., et al., Arctic ocean sciences from submarines—A report based on the SCICEX 2000 Workshop, *Tech. Rep.*, Appl. Phys. Lab., Univ. of Wash., 1999.

Smith, W. H. F., On the accuracy of digital bathymetric data, *J. Geophys. Res.*, *98*, 9591–9603, 1993.

Smith, W. H. F., and P. Wessel, Gridding with continuous curvature splines in tension, *Geophysics*, *55*, 292–305, 1990.

Soluri, E. A., and V. A. Woodson, World vector shoreline, *Int. Hydrol. Rev.*, *67*(1), 27–36, 1990.

U.S. Geological Survey, GTOPO30 digital elevation model, EROS Data Cent., Sioux Falls, S.D., 1997.

Varma, H., H. Boudreau, and W. Prime, A data structure for spatiotemporal databases, *Int. Hydrol. Rev.*, *67*, 71–92, 1990.

Verhoef, J., W. R. Roest, R. Macnab, and J. Arkani-Hamed, Magnetic anomalies of the Arctic and North Atlantic Oceans and adjacent land areas, *Open File Tech. Rep. 3125*, Geol. Surv. of Can., Ottawa, 1996.

Wells, D. E., et al., *Guide to GPS Positioning*, Canadian GPS Associates, Fredricton, N.B., Canada, 1986.

Wessel, P., and W. H. F. Smith, Free software helps map and display data, *Eos Trans. AGU*, 72(41), 441, 445–446, 1991.

B. Calder, M. Jakobsson, and L. Mayer, Center for Coastal and Ocean Mapping, University of New Hampshire, Durham, NH 03824, USA. (brc@ccom.unh.edu; martin.jakobsson@unh.edu; larry.mayer@unh.edu)